Reply on RC1

In the responses below the reviewers' comments are in black and our responses are in red.

The paper presents well-structured research with appropriate methods, results, and scientific soundness. The combined use of different-wavelength SAR, together with car-based SAR, is an important added value. However, some minor revisions are needed to be published, especially for the quality of the figures and some other minor issues that could be improved.

We thank the reviewer for their positive comments and constructive suggestions regarding our manuscript. In the responses below, we address these suggestions and explain the changes we will make to the manuscript.

General comments

Monte mater: EGMS, it could also be possible to also add the dataset 2019 - 2023 (or 2020-2024 if it will be published) to have a long time series for comparison

We did our analyses at Monte Mater with EGMS data from 2018 to 2022 last accessed on 22 April 2025. Currently, EGMS data from 2019 to 2023 can be also accessed. However, a quick visual comparison of the two solutions does not indicate a clear improvement in spatial coverage or a change in the rate of motion. On the contrary, EGMS data from 2018 to 2022 are better in terms of spatial coverage, thus allowing a more conservative estimate of the advantages of L-band versus C-band multi-temporal data. Therefore, updating Fig. 4 and Fig. 12 with the new EGMS solution does not seem to provide added value and would not change our conclusions.

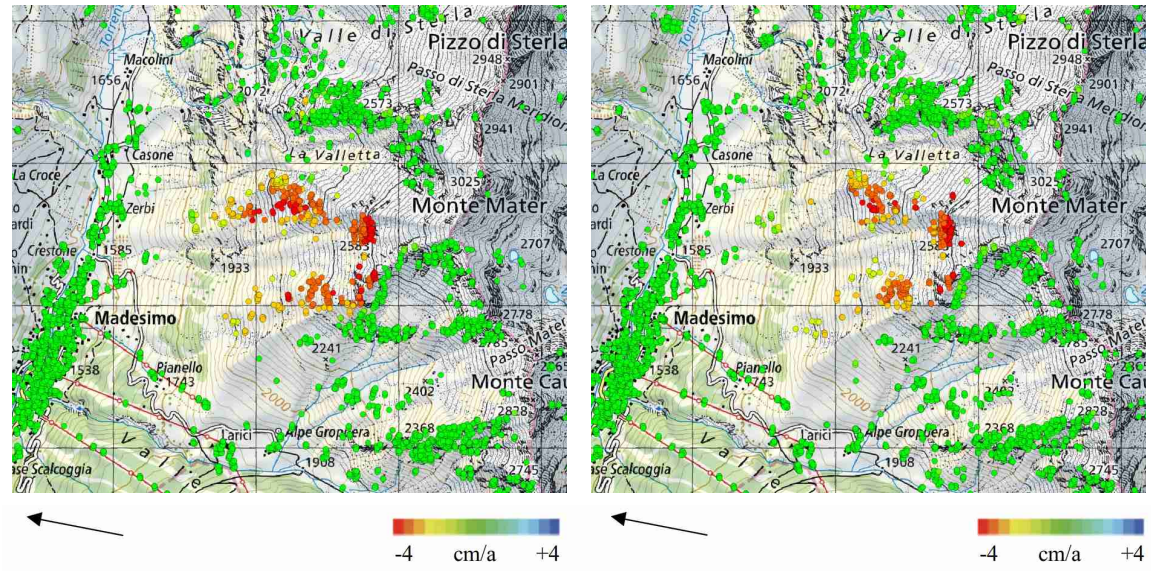

Results of PSI analysis at Monte Mater with Sentinel-1 for the time period 2018–2022 from the European Ground Motion Service (left; EGMS; https://egms.land.copernicus.eu/; last accessed 22 April 2025) and Sentinel-1 for the time period 2019–2023 from the European Ground Motion Service (right; EGMS; https://egms.land.copernicus.eu/; last accessed 5 January 2026). The arrows indicate the satellite LOS direction for the descending orbit. Image background is the Swiss National Map.

Regarding the time series analysis of Fig. 13, there are no EGMS data points between 2019-2023 in a circular sampling area of 50m radius around GB DInSAR pt. 7. Concerning GNSS pt. 800, the time-series plots of the EGMS data between 2018-2022 and 2019-2023 are very similar, without any change of rate in 2023. So again, we believe that updating Fig. 13 with Sentinel-1 PS points derived from Sentinel-1 in Monte Mater between 2019 and 2023 would not change our results.

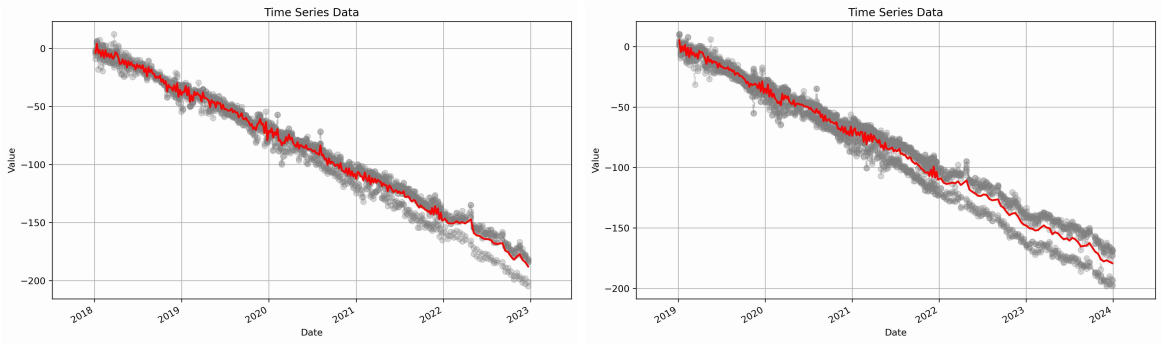

Time series of line-of-sight displacements, extracted and averaged in circular sampling areas (R=50m), for the shallow debris slide in the upper part of the Monte Mater DSGSD at GNSS pt. 800, moving at long-term rates >20 cm/a, for Sentinel-1 for the time period 2018–2022 from the European Ground Motion Service (left; EGMS; https://egms.land.copernicus.eu/; last accessed 22 April 2025) and Sentinel-1 for the time period 2019–2023 from the European Ground Motion Service (right; EGMS; https://egms.land.copernicus.eu/; last accessed 5 January 2026) .

Brienz/Brinzauls: Maybe it is possible to compare the data for DIC/Lidar used in Manconi et al., 2024, as well?

Manconi et al. (2024) jointly considered digital image correlation (DIC) on high-resolution multi-temporal digital terrain models (DTM) generated from airborne surveys as well as InSAR results generated from Sentinel-1 to compute 3-D surface deformation fields. They considered multi-temporal DTMs generated from airborne LiDAR surveys in the period between 2015 and 2020 and presented DIC results for the East-West and North-South directions for 2015–2018 and 2018–2020 (Figure S10).

Our DInSAR stacking analysis using ascending SAOCOM-1 and descending ALOS-2 PALSAR-2 data is from 2024 (Fig. 10) and the GLSAR and ALOS-2 PALSAR-2 interferograms of Fig. 11 are from 2023. Therefore, we believe that validating our latest results with those from older DIC/Lidar measurements would not be an accurate comparison given the large changes in kinematics still ongoing at Brienz/Brinzauls. In addition, using the DIC/LiDAR together with SAOCOM-1 and ALOS-2 PALSAR-2 DInSAR stacking results to compute 3-D surface deformation fields would not be considered innovative.

There is, however, good overall agreement between the DIC/LiDAR results along the north-south direction in 2018-2020 and the GLSAR interferogram in Figure 11. In Section 5.3 (Brienz/Brinzauls, Grisons, Switzerland), we will therefore add a statement about the general agreement of the GLSAR interferogram with DIC data used in Manconi et al. (2024): “The GLSAR interferogram also corresponds very well with the results of digital image correlation (DIC) on high-resolution multi-temporal digital terrain models (DTM) created from airborne surveys along the north-south direction (Manconi et al., 2024).”

It is possible to resume in a table for each satellite and orbit the mean azimuth and incidence angle.

Agreed, a table with the mean azimuth and incidence angles for each satellite and area of interest will be included in the revised manuscript. lv_theta is the SAR look vector incidence angle and lv_phi is the SAR look vector orientation angle (0° → East, 90° → North).

Site	Sensor	lv_theta	lv_phi
Monte Mater	ALOS-2 PALSAR-2 A199-F2-7	41.8°	-170.5°
Monte Mater	ALOS-2 PALSAR-2 D095-F2-5	33.5°	-10.7°

Monte Mater	SAOCOM-1 Asc S3 T214	31.8°	-169.1°
Monte Mater	SAOCOM-1 Desc S4 T112	36.2°	-10.4°
Val Canaria	ALOS-2 PALSAR-2 A199-F2-7	38.9°	-170.0°
Val Canaria	ALOS-2 PALSAR-2 D095-F2-6	37.6°	-10.2°
Val Canaria	SAOCOM-1 Asc S4 T215	36.3°	-169.6°
Val Canaria	SAOCOM-1 Desc S3 T113	32.0°	-10.9°
Brienz/Brinzauls	ALOS-2 PALSAR-2 A199-F3-8	43.5°	-170.7°
Brienz/Brinzauls	ALOS-2 PALSAR-2 D095-F2-5	32.8°	-10.8°
Brienz/Brinzauls	SAOCOM-1 Asc S3 T214	33.4°	-169.3°
Brienz/Brinzauls	SAOCOM-1 Desc S4 T112	35.3°	-10.5°

A table or some consideration showing the max (theoretical) velocity (along LOS) that can be detected by each satellite (I suppose based on acquisition frequency and wavelength) could help visualise the different satellites' upper limits.

We assume that the reviewer is referring in particular to the work of Manconi (2021), in which the temporal phase aliasing thresholds for currently available SAR satellites were calculated based on their nominal wavelengths and revisit times. This refers to the case where the displacement of the target under investigation exceeds the threshold value of $\lambda/4$ between two consecutive satellite acquisitions. Based on these assumptions, the following theoretical velocity thresholds for standard DInSAR are calculated for the three satellite missions and the three GLSAR campaigns considered in our work:

Sensor	Frequency [Hz]	Wavelength [m]	Interval [days]	Threshold [m/year]
PALSAR-2	1.24E+09	0.243	14	1.582
SAOCOM-1	1.28E+09	0.235	16	1.342
GLSAR	1.30E+09	0.231	7	3.010
GLSAR	1.30E+09	0.231	82	0.257
GLSAR	1.30E+09	0.231	239	0.088

For the DInSAR stacking analysis at Brienz (Fig. 10), 28 days ALOS-2 PALSAR-2 were also considered. For the SBAS analysis at Val Canaria with SAOCOM-1 (Fig. 8), acquisition time intervals of maximum 270 days were considered. For PSI, only summer data without snow cover were mainly used and in these cases we might therefore consider acquisition time intervals of maximum 365 days (i.e., from one summer to the next). Based on these assumptions, the following theoretical velocity thresholds are further calculated:

Sensor	Frequency [Hz]	Wavelength [m]	Interval [days]	Threshold [m/year]
Sentinel-1	5.41E+09	0.056	365	0.014
PALSAR-2	1.24E+09	0.243	28	0.791
PALSAR-2	1.24E+09	0.243	365	0.061
SAOCOM-1	1.28E+09	0.235	270	0,080
SAOCOM-1	1.28E+09	0.235	365	0,059

We agree to include such a table as Appendix D in the revised version of the manuscript. We will then make reference to this table in the discussion of Section 6.2 Monitoring Performance.

For the PS density calculation, it would be better to show where the area is in which PS is calculated, and to include a land use map to better understand what is classified as forest and non-

forest. For the plot, use the same scale for A B and C, at least using log axis Y to evidence the different order of density from C to L band

We agree with the reviewer that a land use map showing the area in which the PS density of Figure 12 was calculated would be helpful in better understanding what is classified as forest and non-forest. We have created such maps in our project, but for the paper we had to summarize the most important results in a reasonable number of figures and therefore did not include them. We currently have 13 figures, which is already at the upper end of the scale. To get an idea of how much forest area there is at each site, readers can refer to Fig. 1, which shows pictures of the three study areas. However, to better assess the size of the area in which PS density is calculated and how much of it is forest and non-forest, we will add these numbers in the revision of section 6.1 L-band versus C-band.

Site	Total area [km2]	Non-forested area [km2 / %]	Forested area [km2 / %]
Monte Mater	3.21	2.94 / 92%	0.27 / 8%
Val Canaria	3.88	1.45 / 37%	2.44 / 63%
Brienz/Brinzauls	3.12	2.15 / 69%	0.97 / 31%

In addition, in Appendices A to C we will add maps with the boundaries of the mapped landslides, the forest cover from the CORINE Land Cover (CLC) and shaded reliefs of the DEMs, see first comment about the figures below.

Using the same logarithmic scale for the three plots in Figure 12 to evidence the different order of density from C- to L-band at the three sites is certainly a valuable option. We will do this when revising the manuscript.

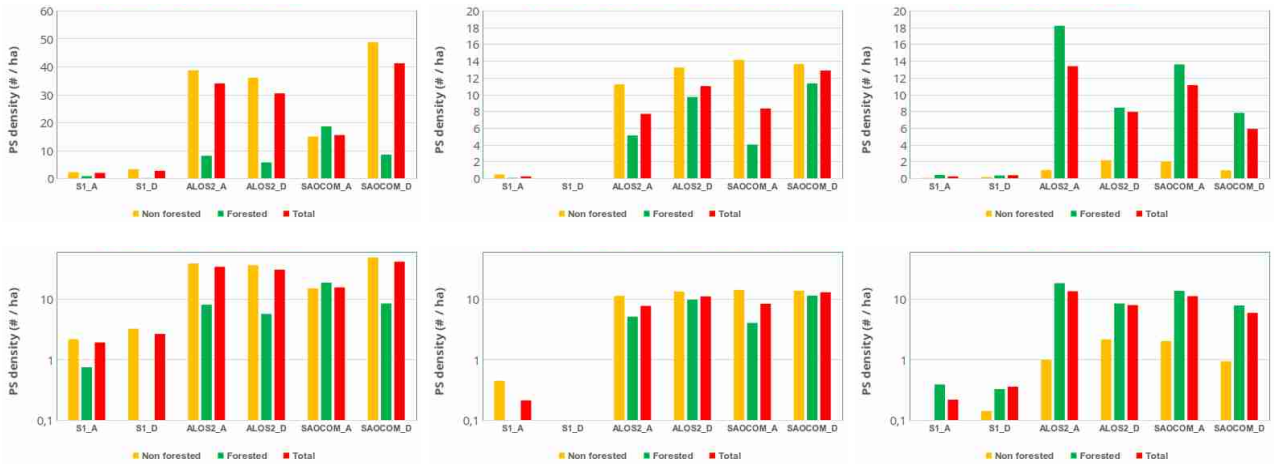

PS densities for products derived from Sentinel-1 (S1), ALOS-2 PALSAR-2 (ALOS2) and SAOCOM-1 (SAOCOM) in ascending (A) and descending (D) orbits in non-forested, forested and total SAR-visible areas for (left) the Monte Mater, (middle) the Val Canaria and (right) the Brienz areas. The upper row uses a different linear scale, the second row uses the same logarithmic scale.

Specific comments

Line 133: collapse on 27 October 2009 (any reference)

No, unfortunately there are no scientific papers describing this event.

Line 194 : as shown in Fig. 6 is 3 ?

Correct, Fig. 3. This will be changed in the revision. Thank you for spotting this mistake.

Figures

Where possible, add the boundaries of DSGSD and landslide/, especially when interferograms cover the entire area.

Here we face two problems. On the one hand, we already have a comprehensive manuscript with many descriptions and illustrations, which are at the upper limit of what we consider appropriate for a research paper. On the other hand, slope instabilities, as shown in the following images, were not classified at our three test sites using a similar methodology. If we were to show the boundaries of slope instabilities in the displayed interferograms, we would have to add a detailed description of the delineation process. This would take up a large part of the overall description, as the inventories are not published and thus cannot be referred to. Furthermore, we also believe that the moving areas in the interferograms are already clearly visible without the need for additional markings. Due to these reasons, we prefer not to discuss the inventory of slope instabilities in our current manuscript. Nevertheless, we will add in Appendices A to C the following three maps with the boundaries of the mapped landslides, the forest cover from the CORINE Land Cover (CLC) and shaded reliefs of the DEMs, see first comment about the figures below.

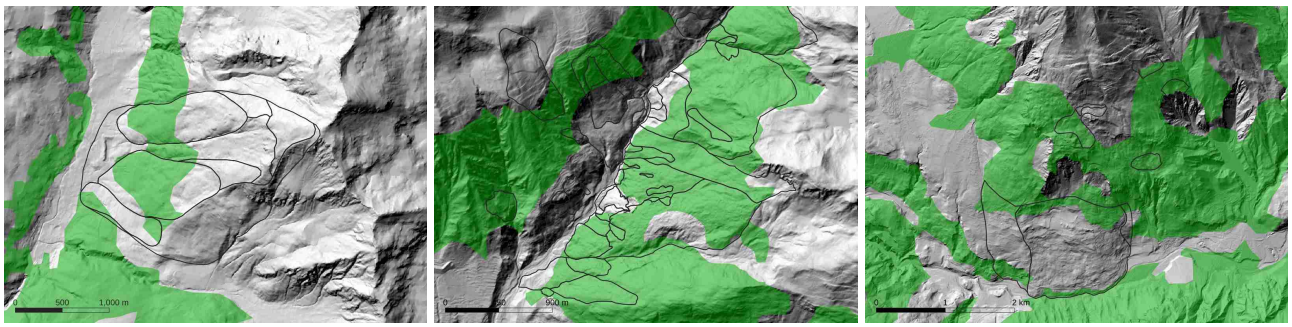

Left) Kinematic domains of the Monte Mater large landslide complex (Crippa et al., 2020). Middle) Slope instabilities map of the Val Canaria area of interest (De Pedrini et al., in preparation). Right) Landslide hazard indication map over the Brienz/Brinzauls AOI (Geoportal Kanton Graubünden, https://map.geo.gr.ch, last accessed 27 February 2026). The forest cover from the CORINE Land Cover (CLC) is shown in green, background is the shaded reliefs of the DEM.

In some figures (e.g., 6), the aerial photo appears to have a black pixel; is it a shadow mask? If yes, add to the legend.

Correct, in some of the images layover/shadow is shown in black or dark grey. This will be specified in the caption to the figures in the revised version of the manuscript.

Figure 4 and others: Please add scale and coordinates

Agreed, we will add the geographical coordinates to the figures. In addition, for images that use the Swiss national map as a background, we will make it clear that the grid spacing is 1 km.

Figure 8: Please use the same scale of velocity displacement

Figure 8 shows two distinct analyses. The image on the left shows the velocity of a SBAS analysis from ascending SAOCOM-1 for the time period 2020–2024 expressed in cm/a. The image on the right shows a car-borne GLSAR LOS displacement map between 3 July and 23 September 2024 expressed in cm. Therefore, we use different scales for the velocity and the displacement.

Figure 12: move at the end of par 6.1

Agreed. This figure will be moved to the end of section 6.1, formatting permitting.